Neutron Shell Structure in ^{91}Zr and ^{92}Zr by (d,p) and $(\alpha, {}^3\mathrm{He})$ Reactions*

C. R. Bingham
The University of Tennessee, Knoxville, Tennessee 37916
and Oak Ridge National Laboratory, Oak Ridge, Tennessee 37830

and

M. L. Halbert
Oak Ridge National Laboratory, Oak Ridge, Tennessee 37830

(Received 13 May 1970)

Angular distributions from ~12.5 to ~45° were measured for ^{90}Zr(d,p) and ^{91}Zr(d,p) at 33.3 MeV. The resolution was about 25 keV. A number of doublets were resolved, and levels were found that had not been reported in previous neutron-transfer studies. ^{90}Zr$(\alpha, {}^3\mathrm{He})$ and ^{91}Zr$(\alpha, {}^3\mathrm{He})$ spectra with 55-keV resolution were obtained at 15 and 20° with 65.9-MeV α particles. The data are compared with distorted-wave predictions. The (d,p) spectroscopic factors agree with those from the $(\alpha, {}^3\mathrm{He})$ reaction wherever comparisons are feasible. Sums of spectroscopic factors, centers of gravity, and second moments are presented for levels assigned to $d_{5/2}$, $s_{1/2}$, $d_{3/2}$, $g_{7/2}$, and $h_{11/2}$ configurations in each final nucleus. The sums are generally in agreement with the sum-rule predictions. The $h_{11/2}$ strength appears to be highly fragmented; in both nuclei, about 50% of the predicted strength was identified. The separations of the centers of gravity are similar for the two nuclei.

I. INTRODUCTION

The neutron shell structure in the isotopes of Zr has previously been studied by (d,p) reactions at bombarding energies between 2.7 and 17 MeV.[1-5] From $(\alpha, {}^3\mathrm{He})$ at 65-MeV bombarding energy,[6] it became apparent that either much information was missed in the (d,p) experiments or else the distorted-wave theory for $(\alpha, {}^3\mathrm{He})$ reactions was grossly in error. Recent experimental data[7] on ^{116}Sn$(\alpha, {}^3\mathrm{He})$ gave spectroscopic factors for $l=0$, 2, 3, 4, and 5 similar to those from ^{116}Sn(d,p), thus showing that the distorted-wave calculations were probably not responsible for the discrepancies between the Zr results. It appeared that a more comprehensive study of the neutron shell structure in Zr was needed, especially for the high-l shells. To enhance the high-l transfers, an energy considerably higher than 17 MeV is desirable. Since optical-model parameters describing the elastic scattering of 34-MeV deuterons[8] and 30- and 40-MeV protons[9] are available, a bombarding energy near 34 MeV was selected.

The earlier (d,p) experiments[1-5] were carried out with an energy resolution of 40–100 keV. The present work was done with 25-keV resolution. A number of levels unresolved or unreported in the earlier (d,p) experiments were observed.

The earlier $(\alpha, {}^3\mathrm{He})$ measurements[6] were done with relatively poor resolution (~200 keV). To help clarify the experimental situation, especially with regard to weak $l=5$ transfers, additional $(\alpha, {}^3\mathrm{He})$ spectra at 65.9 MeV were obtained at 15 and 20° with a resolution of 55 keV.

II. EXPERIMENTAL DETAILS

The deuterons and α particles used in this experiment were accelerated by the Oak Ridge Isochronous Cyclotron to energies of 33.3 and 65.0 MeV, respectively. The beams were energy-analyzed by a 153° $n=\frac{1}{2}$ magnet with a 72-in. radius of curvature.

The protons and ^{3}He particles were recorded with 50-μ Kodak NTB emulsions placed in the focal plane of the broad-range spectrograph[10] with an acceptance angle of 3°. The proton and ^{3}He plates were scanned in $\frac{1}{4}$- and $\frac{1}{2}$-mm strips, respectively. For the proton spectra all other particles were absorbed with a 0.040-in. Al absorber in front of the plate. The protons and deuterons could not be removed from the ^{3}He spectra by absorbers. However, the ^{3}He are much more highly ionizing, and by judicious development of the plates, background due to deuterons and protons was minimized. The competing deuterons resulted from (α, d) reactions to residual states of ~30-MeV excitation, and hence probably contributed only a smoothly varying background.

The ^{90}Zr and ^{91}Zr targets are rolled foils of thickness 1.20 and 0.54 mg/cm^2, respectively. The energy loss of ^{241}Am α particles when penetrating the targets was measured. The thicknesses were determined by interpolation in the range-energy tables of Whaling.[11] The foils were found to be uniform within 10%. The ^{90}Zr target is 98.6%

^{90}Zr, 0.8% ^{91}Zr, 0.4% ^{92}Zr, and 0.2% ^{94}Zr. The ^{91}Zr target is 5.0% ^{90}Zr, 90.9% ^{91}Zr, 3.3% ^{92}Zr, 0.8% ^{94}Zr, and 0.2% ^{96}Zr.

The incident beam was collected in a Faraday cup, and absolute cross sections were calculated. The accuracy of the cross sections was limited mainly by uncertainty in the target thickness and efficiency of the plate scanners. The over-all error in the cross sections is about ±15%.

The spectra for ^{90}Zr(d, p) at 22.5°, ^{91}Zr(d, p) at 17.5°, ^{90}Zr$(\alpha, ^3\text{He})$ at 15°, and ^{91}Zr$(\alpha, ^3\text{He})$ at 15°, all in the lab system, are shown in Figs. 1–4, re-

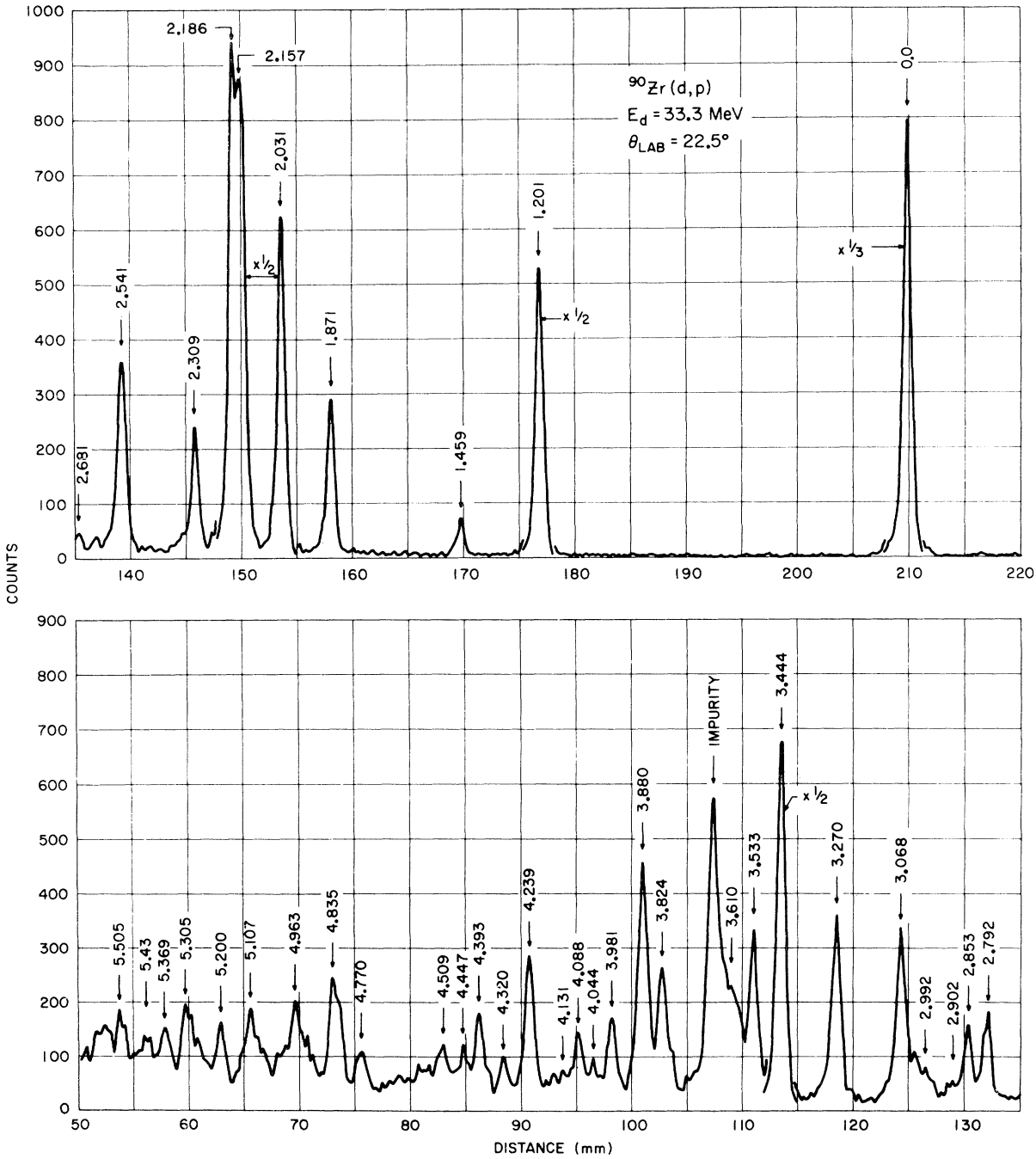

FIG. 1. The ^{90}Zr(d,p) spectrum at 22.5° lab. The excitation energies of the residual states are given for the prominent transitions.

spectively. The over-all resolution for the proton spectra is about 25 keV and that of the ^{3}He spectra is about 55 keV.

Angular distributions of the proton groups were obtained from 12.5 to 42.5° lab for comparison with distorted-wave predictions. The ^{3}He spectra were obtained at only 15 and 20° for the ^{90}Zr target and at 15, 17.5, and 20° for the ^{91}Zr target, since the structure in (α, ^{3}He) angular distributions is known to be weak.[6]

III. METHOD OF ANALYSIS

Distorted-wave calculations were made with the program JULIE[12] for both the (d, p) and (α, ^{3}He) cross sections. The details of the calculation are discussed below. The distorted-wave cross section is given by

$$\frac{d\sigma}{d\Omega} = \frac{NR}{2s+1}\,\frac{2J_f+1}{2J_i+1}\,S\sigma_{\mathrm{JULIE}}(\theta),$$

where J_i and J_f are the spins of the target and residual nuclei, respectively, $s=\frac{1}{2}$ is the spin of the stripped neutron, S is the spectroscopic factor, and NR accounts for the overlap of the ingoing particle and the outgoing particle-neutron system, as well as the strength of the interaction causing the transition. By using a Hulthén wave function for the deuteron, one obtains a value of $NR=3.00$

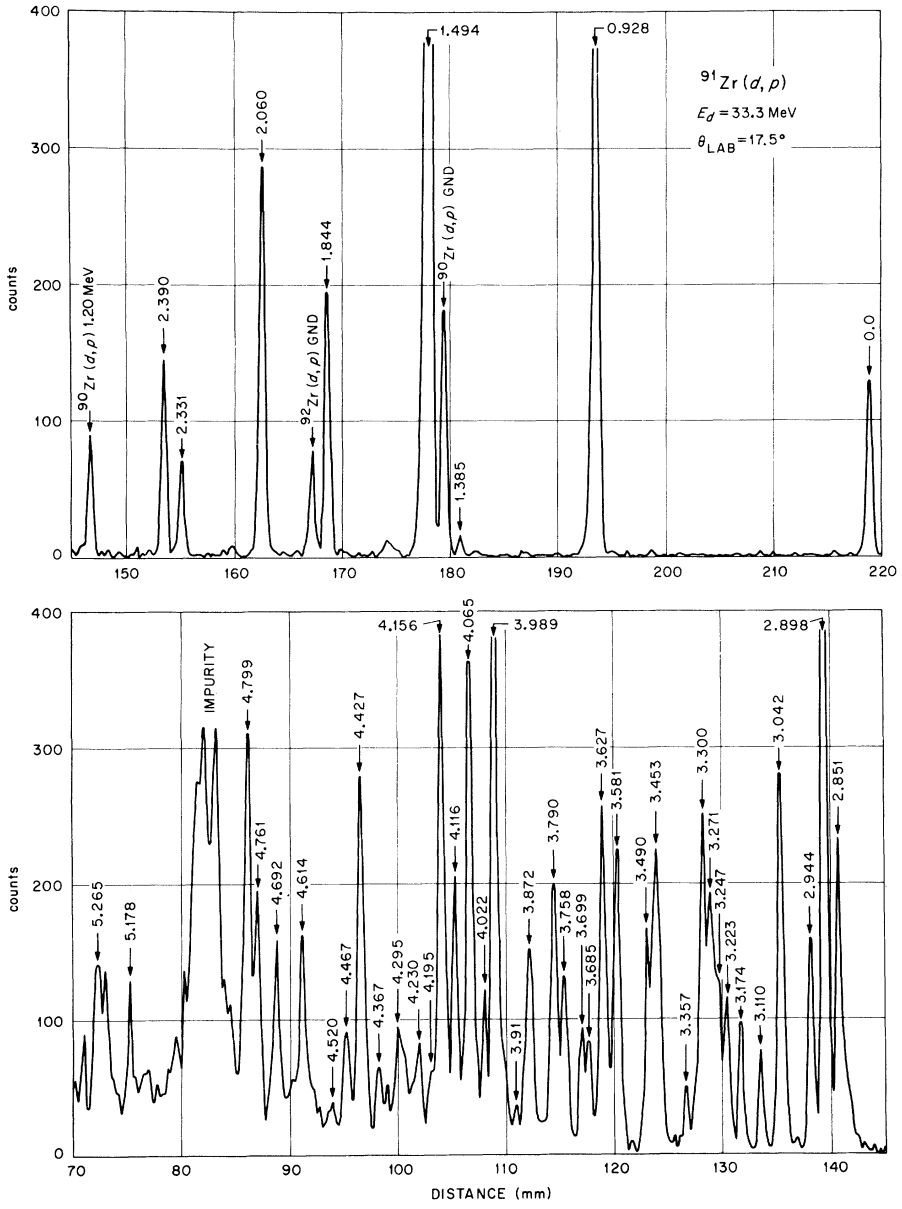

FIG. 2. The ^{91}Zr(d, p) spectrum at 17.5°. The excitation energies of the residual states are given for the prominent transitions. The peaks at 3.490, 3.581, and 3.627 MeV contain significant contributions from ^{90}Zr(d, p) to levels of ^{91}Zr at 2.03, 2.16, and 2.19 MeV.

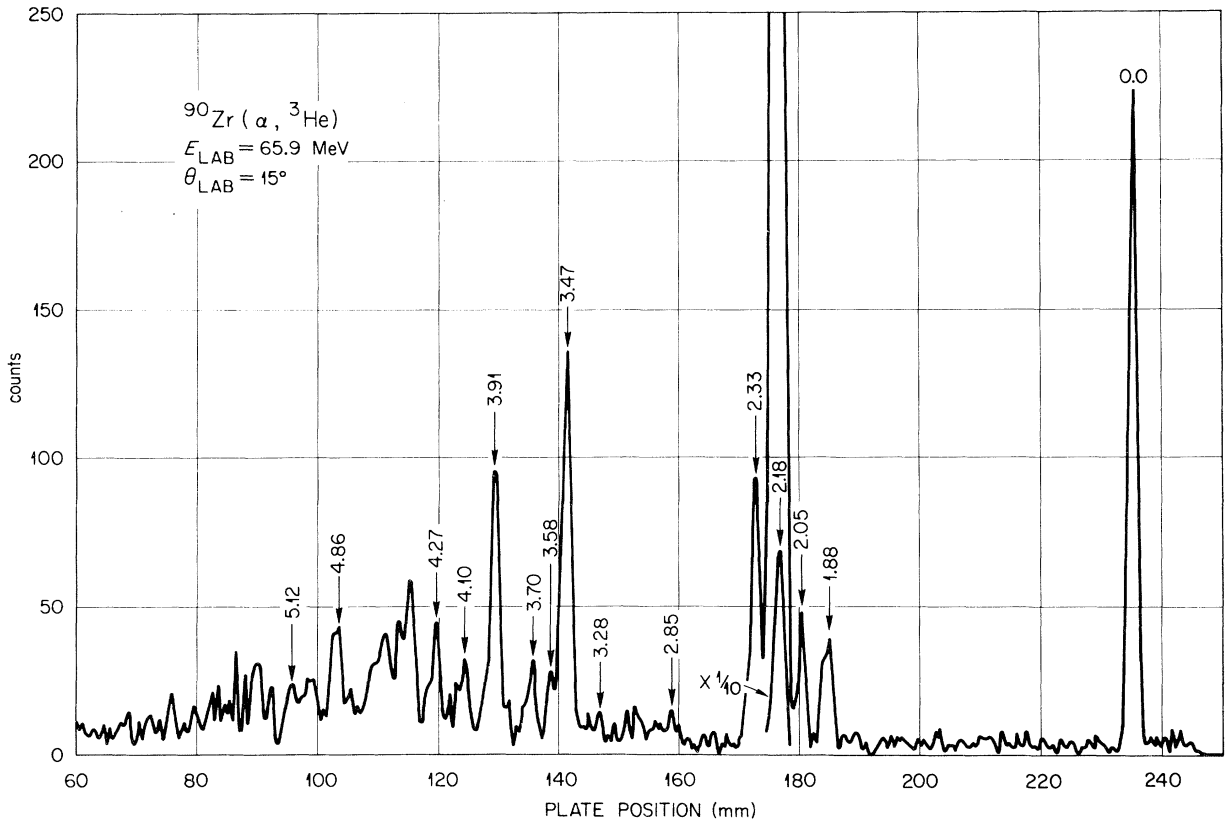

FIG. 3. The ^{90}Zr(α, ^{3}He) spectrum at 15° lab. The excitation energies of the residual nuclei are given for the prominent transitions.

for the (d, p) reaction.[13] This value was used in the present work. The value of $NR = 92.1$ used here for the $(\alpha, {}^3\mathrm{He})$ reaction was obtained empirically in previous work.[14] It is in good agreement with a theoretical prediction by Bassel,[15] but it differs by a factor of 12 from a prediction by Lim.[16]

A. (d,p) Reaction

The distorted-wave calculation for the (d, p) cross sections employed nonlocal potentials[17] for the ingoing and outgoing channels and finite-range effects in the local energy approximation.[18] No radial cutoffs were used. The range used for the deuteron and proton channels was 0.54 and 0.85 F, respectively. The range of the interaction was taken to be 1.54 F. The nonlocality and finite-range corrections were made by multiplying the local form factor by appropriate corrective functions.[17,18] The local form factor is the radial bound-state wave function of the stripped neutron. It is taken as the solution of Schrödinger's equation for a Woods-Saxon potential with a spin-orbit

TABLE I. Optical-model potentials used in the distorted-wave calculations. The Coulomb potential was taken to be that of a uniformly charged sphere of radius $1.25A^{1/3}$ F for protons, $1.30A^{1/3}$ F for deuterons, and $1.40A^{1/3}$ F for the He ions.

Particle	V_0 (MeV)	W_0 (MeV)	W_D (MeV)	V_s (MeV)	r_0 (F)	a_0 (F)	r_0' (F)	a_0' (F)	r_s (F)	a_s (F)
d	98.53 [a]	0	13.52	6.53	1.093	0.800	1.287	0.817	r_0	a_0
p	48.8 [b]	5.31	2.95	6.04	1.16	0.75	1.37	0.63	1.064	0.738
^{3}He	196.9 [c]	17.37			1.04	0.811	1.60	0.797		
^{90}Zr+α	100.0 [d]	38.0			1.401	0.646	r_0	a_0		
^{91}Zr+α	100.0 [d]	45.0			1.390	0.661	r_0	a_0		

[a] Potential for ^{91}Zr(d,d), Ref. 8.
[b] Interpolated from potentials of Ref. 9.
[c] Potential A of Ref. 14.
[d] Read from Fig. 15, Ref. 6.

term of the Thomas form having $r_0 = 1.24$ F, $a = 0.65$ F, $r_{0s} = 1.14$ F, $a_s = 0.65$ F, $\lambda = 25$, and a well depth adjusted to give an eigenvalue equal to the binding energy of the transferred neutron. The geometry of the spin-orbit term given by r_{0s} and a_s was selected by comparison of the geometry of the central term and the spin-orbit term of potentials describing the behavior of polarized protons.[9]

The wave function for the ingoing deuteron was calculated from a potential which describes the elastic scattering of 34-MeV deuterons from ^{91}Zr.[8] Surface absorption was used. The parameters are listed on line 1 of Table I.

The proton energies varied from 33 to 39 MeV. The potential for the proton channel was obtained by interpolation between the potentials which fit elastic scattering and polarization data at 30 and 40 MeV.[9] The "standard" geometry was used, and the well depth V_0 was adjusted according to the formula of Ref. 9. Linear interpolation between the 30- and 40-MeV data was used to determine the volume absorption well depth W_0 and the surface absorption well depth W_d. The parameters at midrange (36 MeV) for ^{91}Zr are listed in Table I, line 2.

B. (α, ^{3}He) Reaction

The (α, ^{3}He) calculations were made in zero range with local potentials. Effects similar to the effects of nonlocality and finite range can be produced by choosing α potentials with deeper absorptive wells. The spin-orbit term of the bound-state potential had the same geometry as the central term, but λ was reduced from 25 to 6.0. It was shown previously[7] that such a procedure gives results very nearly equal to the results with the prescription described above for the (d, p) calculation.

The optical-model parameters used for the ^{3}He and α-particle channels are listed in Table I. They are the ones used in previous (α, ^{3}He) and (^{3}He, α) analyses[6,14] to fit measured angular distributions. A detailed study of the effect of optical-model parameters was made in Refs. 6 and 14. The best choice of α potential, selected from among the many potentials which give adequate fits to the elastic scattering, was found to depend on the ^{3}He potential used. Different pairs of potentials which gave equally good fits to the angular distributions were found to give the same spectroscopic factors.

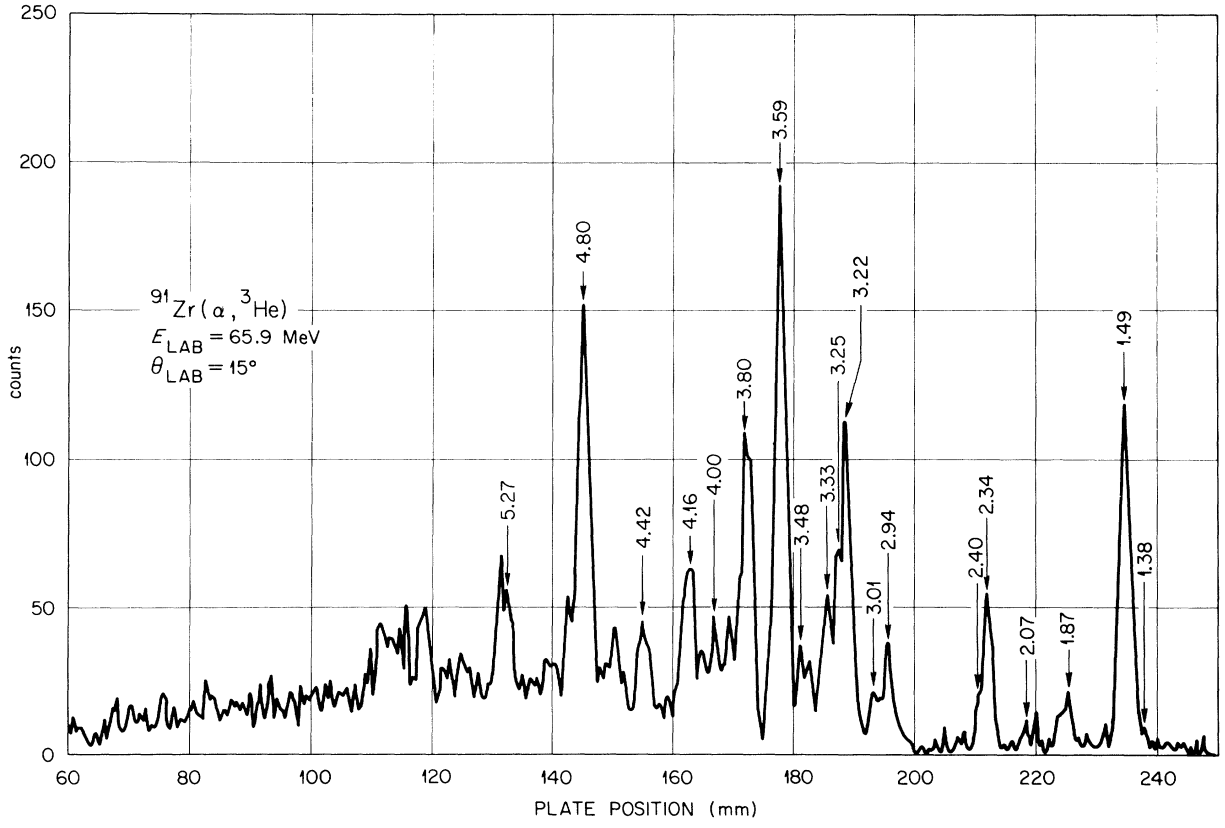

FIG. 4. The ^{91}Zr(α, ^{3}He) spectrum at 15° lab. The excitation energies of the residual nuclei are given for the prominent transitions. The ground-state and 0.928-MeV peaks are not shown.

IV. RESULTS

A. ^{90}Zr Target

The ^{90}Zr(d,p) angular distributions are compared with the distorted-wave predictions in Figs. 5–8. The resulting spectroscopic factors are given in Table II.

The ground state is a $\frac{5}{2}^+$ state. It can be described predominantly as a $d_{5/2}$ neutron coupled to the ^{90}Zr ground state, but it does contain small admixtures of other configurations.[19] Hence, part of the $[d_{5/2}, {}^{90}\text{Zr(g.s)}]$ is located in other levels, and the 1.459-MeV level is probably a $\frac{5}{2}^+$ state. The remainder of the $l=2$ transfers are treated as $d_{3/2}$. The $l=4$ and $l=5$ transitions were treated as $g_{7/2}$ and $h_{11/2}$ transfers, respectively, since the $g_{9/2}$ shell appears to be filled[19] and the $h_{9/2}$ shell is expected to lie at much higher energies.

Although complete angular distributions for $(\alpha, {}^3\text{He})$ were not measured, distorted-wave calculations were made and spectroscopic factors derived. These are also listed in Table II. The spectroscopic factors from $(\alpha, {}^3\text{He})$ agree well with those from (d,p). The states populated by large l transfers are dominant in the $(\alpha, {}^3\text{He})$ spectra, so the $l=0$ cross sections could not be measured to good accuracy. In a few cases doublets were not resolved in the ^{3}He spectrum. For example, the $l=4$ state at 2.186 and the $l=5$ at 2.157 MeV were not separated in the $(\alpha, {}^3\text{He})$ data. In these cases the spectroscopic factor for the lower-l transfer was set equal to the (d,p) result, and the spectroscopic

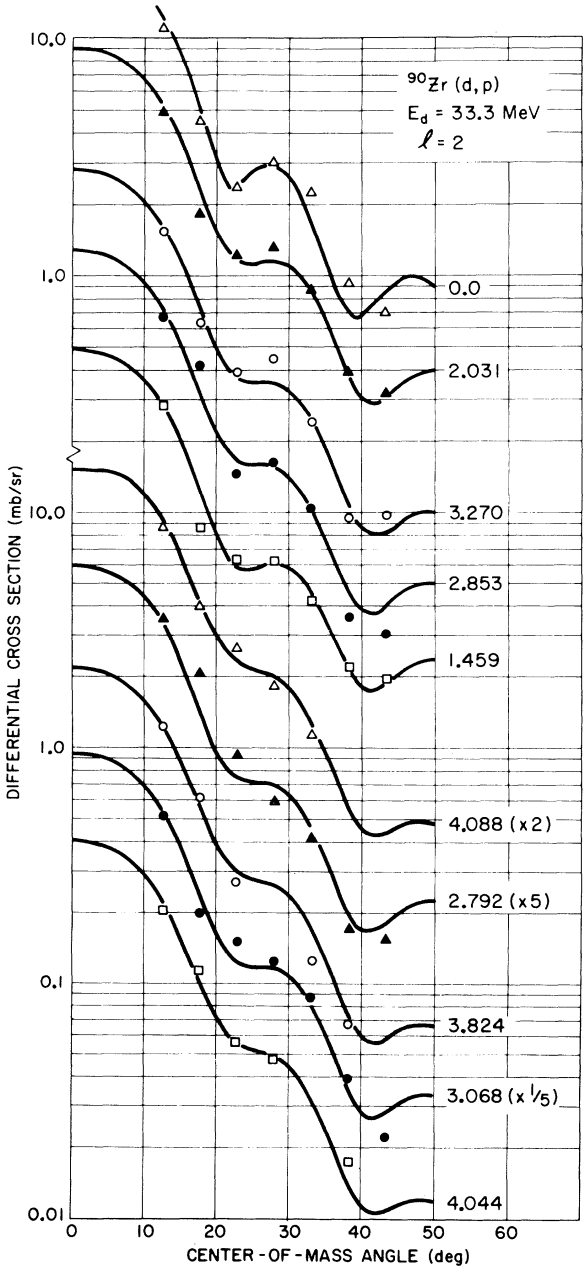

FIG. 5. Experimental angular distributions for $l=2$ transitions in ^{90}Zr(d,p) (points) in comparison with distorted-wave calculations (smooth curves).

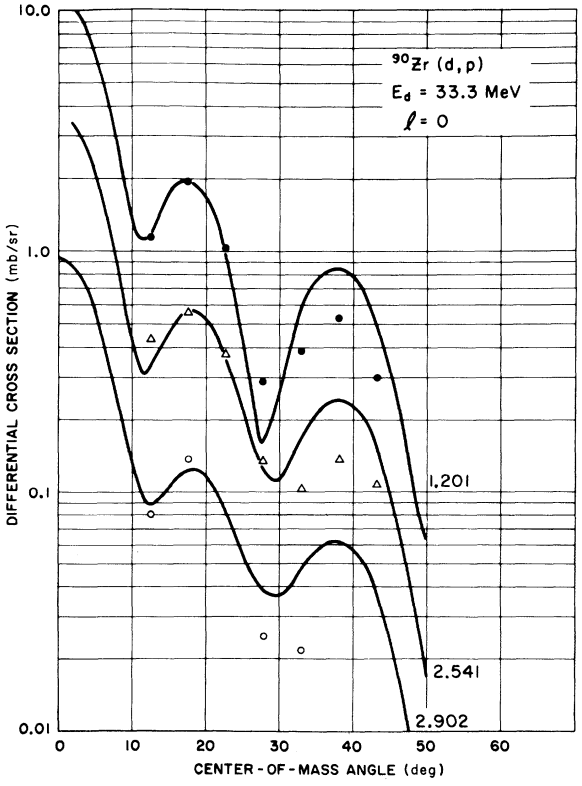

FIG. 6. Experimental angular distributions for $l=0$ transitions in ^{90}Zr(d,p) (points) in comparison with distorted-wave calculations (smooth curves).

factor for the higher spin state was deduced for comparison.

A few spin assignments initially suggested by analysis of the (d, p) data were rejected when a detailed comparison with the $(\alpha, {}^3\mathrm{He})$ data was made. In some cases the peaks are apparently doublets in both the (d, p) and $(\alpha, {}^3\mathrm{He})$ spectra. Two examples of (d, p) angular distributions which must contain some higher-l component in order to agree with $(\alpha, {}^3\mathrm{He})$ are shown in Fig. 8. The higher-l component is dominant in the $(\alpha, {}^3\mathrm{He})$ spectrum. The angular distributions for these groups at 3.661 and 3.880 MeV are compared with a weighted sum of $l=2$ and $l=5$ calculated cross sections. The weights were adjusted to give agreement with the $(\alpha, {}^3\mathrm{He})$ spectroscopic factors. It is clear that these spectroscopic factors could not be found from the (d, p) data alone.

B. ^{91}Zr Target

The angular distributions for ^{91}Zr(d, p) are compared with the distorted-wave predictions in Figs. 9–11. The resulting spectroscopic factors are listed in Table III. For many cases the final spin is unknown and so values of

$$S' = [(2J_f+1)/(2J_i+1)]S$$

are given. The spectroscopic factors from $(\alpha, {}^3\mathrm{He})$ were measured and are listed in Table III, also. The spectroscopic factors from the $(\alpha, {}^3\mathrm{He})$ are in good agreement with the (d, p) results. In a few cases peaks were treated as doublets or configuration-mixed states in order to maintain agreement between the two experiments.

V. DISCUSSION

The spectroscopic factors for each subshell were summed, and the center of gravity of states of each subshell was calculated with the formula

$$\epsilon = \sum_i E_i^* S_i' / \sum_i S_i' .$$

The spread of the levels in each subshell (i.e., the square root of the second moment) was then calculated as

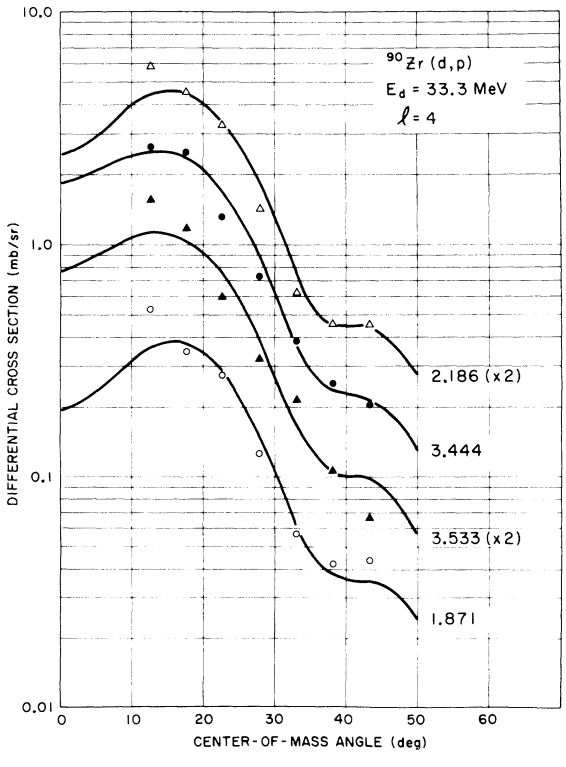

FIG. 7. Experimental angular distributions for $l=4$ transitions in ^{90}Zr(d,p) (points) in comparison with distorted-wave calculations (smooth curves).

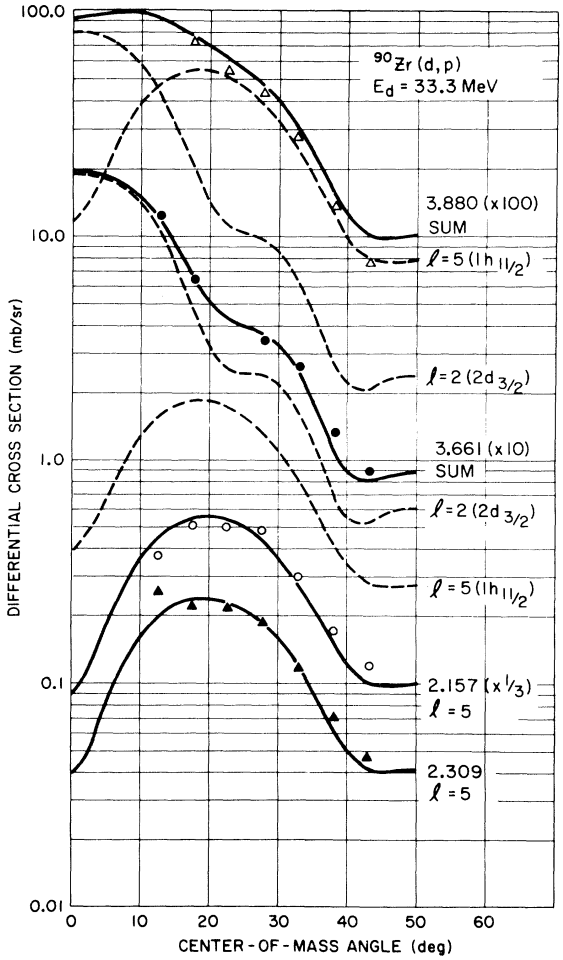

FIG. 8. Experimental angular distributions for peaks containing $l=5$ transitions in ^{90}Zr(d,p) (points) in comparison with distorted-wave calculations (smooth curves).

TABLE II. Excitation energies, spin assignments, and spectroscopic factors for $^{90}Zr(d,p)$ and $^{90}Zr(\alpha,{}^3He)$ in comparison with results from $^{91}Zr(p,p')$ and $^{92}Zr(p,d)$.

Present results $^{90}Zr(d,p)$			Present results $^{90}Zr(\alpha,{}^3He)$		$^{91}Zr(p,p')$ [a]			$^{92}Zr(p,d)$ [b]		
E^* (MeV)	j^π	S	E^* (MeV)	S	E^*	l	j^π	E^*	j^π	C^2S
0.0	$5/2^+$	1.04	0.0	0.98	0.0		$5/2^+$	0.0	$5/2^+$	1.86
1.201	$1/2^+$	0.93			1.21		$1/2^+$	1.204	$1/2^+$	0.06
1.459	$5/2^+$	0.03			1.46		$5/2^+$	1.47		
1.871	$7/2^+$	0.08	1.874	0.087	1.876	2	$9/2^+$			
2.031	$3/2^+$	0.63	2.040	0.45	2.035	2	$5/2^+$	2.04	$3/2^+$	0.07
					2.08		$(3/2)^+$			
					2.123	2	$7/2^+$	2.135	$9/2^+$	0.78
2.157	$11/2^-$	0.37	2.176	0.41	2.162	3	$(11/2)^-$			
2.186	$7/2^+$	0.48		0.48 [c]	2.19		$7/2^+$	2.180	$7/2^+$	0.20
2.309	$11/2^-$	0.048	2.323	0.053						
					2.385		$(3/2)^+$	2.350		
					2.524					
2.541	$1/2^+$	0.34			2.549					
					2.566		$(1/2)^+$			
					2.630		$(1/2)^-$			
2.681					2.683		$(7/2)^-$			
					2.75					
					2.77					
2.792	$(3/2^+)$	0.07			2.800		$(9/2)^-$			
					2.821		$(5/2)^-$			
2.853	$3/2^+$	0.08	2.847	0.13				2.895	$9/2^+$	7.9
2.902	$(1/2^+)$	(0.10)								
					2.92		$(3/2,5/2)^+$			
2.992					3.00	4				
					3.022		$(3/2)^-$			
3.068	$3/2^+$	0.28	3.063	0.22	3.07					
					3.09		$(3/2,5/2)^+$			
					3.22			3.225	$(1/2,3/2)^-$	1.00, 0.91
3.270	$3/2^+$	0.17	3.277	0.19	3.27					
					3.30					
3.444	$7/2^+$	0.42	3.466	0.34	3.46			3.468	$(1/2,3/2)^-$	0.82, 0.76
					3.48					
3.533	$7/2^+$	0.09	3.575	0.08	3.56			3.567	$(1/2,3/2)^-$	1.14, 1.04
3.610										
3.661	$(3/2^+,11/2^-)$	(0.11, 0.028 [d])	3.676	(0.11 [c], 0.028)	3.64					
3.721					3.69					
					3.74					
					3.80					
3.824	$(3/2^+)$	0.12	3.817	0.19	3.84					
3.880	$(3/2^+,11/2^-)$	(0.045, 0.08 [d])	3.904	(0.045 [c], 0.085)				3.890		
	$(11/2^-)$ [e]		4.081	0.035						
	$(11/2^-)$ [e]		4.254	0.056						

[a] See Ref. 21.
[b] See Ref. 19
[c] Set equal to (d,p) result.
[d] Set approximately equal to $(\alpha,{}^3He)$ result.
[e] Assigned on basis of $(\alpha,{}^3He)$.

$$\bar{\sigma} = \left[\sum_i (E_i^* - \epsilon)^2 S_i' / \sum_i S_i' \right]^{1/2}.$$

These are listed in Table IV for both residual nuclei. The spectroscopic-factor sums for the $s_{1/2}$ and $d_{3/2}$ levels are somewhat higher than the sum-rule limit. This may indicate that some of the groups given these assignments are actually very complex and are perhaps excited in other ways. The level spacing is such that more than one level

is perhaps included in some groups. Part of the difficulties could be resolved by an over-all renormalization of the spectroscopic factors. Indeed, some preference for a normalization factor of 3.30 (instead of 3.00) for (d, p) calculations has been expressed.[20] This would reduce the spectroscopic factors by 10%.

A. Residual Nucleus ^{91}Zr

The center of gravity of the $h_{11/2}$ states observed is lower than one would expect in Zr. However, the sum of the spectroscopic factors for $h_{11/2}$ transitions is also low, perhaps indicating that much strength lies at higher energies. The remaining strength appears to be highly fragmented. A $h_{11/2}$ transition with a large spectroscopic factor would certainly produce a large peak in the $(\alpha, {}^3\mathrm{He})$ spectrum. No other large peaks were observed up to about 5.5 MeV.

Except for the $d_{5/2}$ transitions, which are dominated by the ground-state transition, the values of $\bar{\sigma}$ for the levels in different subshells are very nearly equal (0.7 MeV).

Also shown in Table II are the results of ^{91}Zr(p, p)[21] and ^{92}Zr(p, d)[19] experiments. The spins proposed in Ref. 21 from the inelastic scattering data result from an analysis in terms of a core-excitation model. In a few cases the distorted-wave analyses of the transfer reactions suggest different assignments. The 1.871-MeV level is almost certainly a $\frac{7}{2}^+$ level, since it is populated in (d, p) and not in (p, d). Likewise, the level at 2.031 is $\frac{3}{2}^+$ and the one near 2.13 MeV must be $\frac{9}{2}^+$.

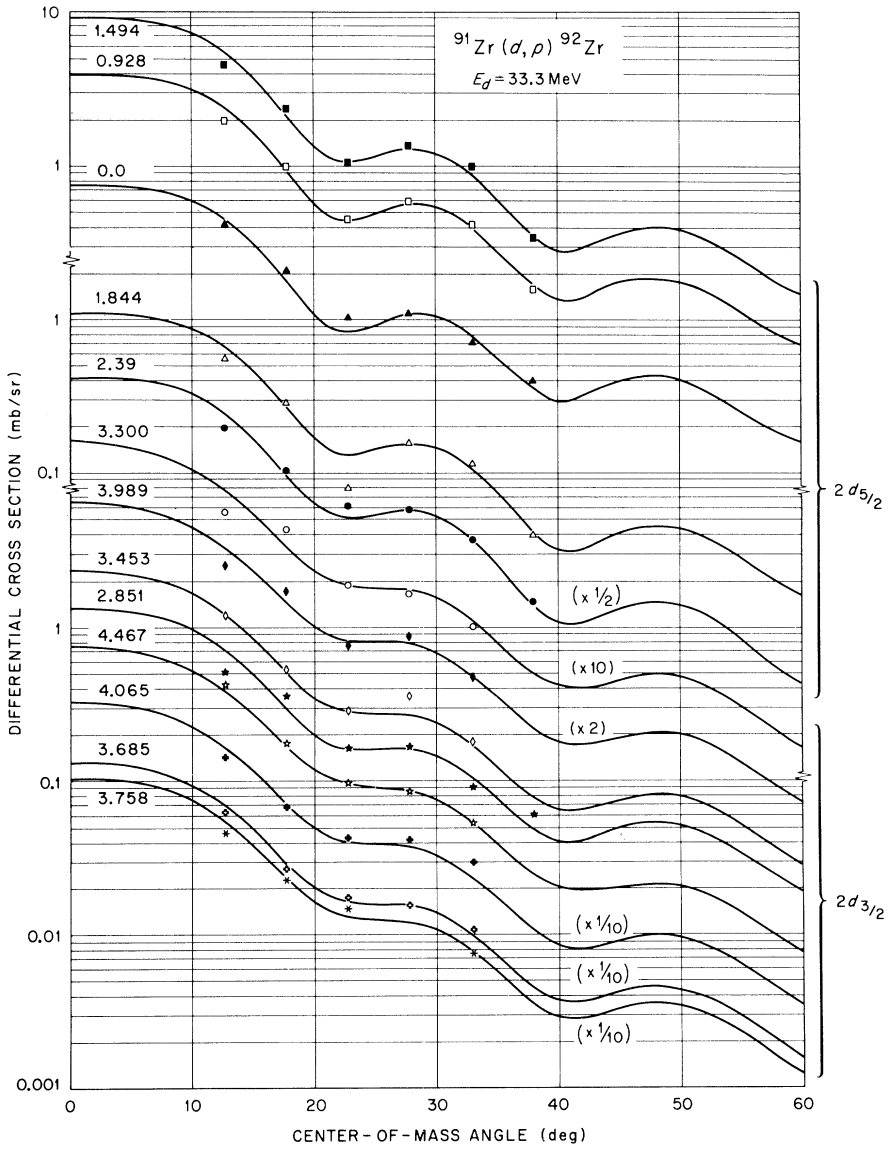

FIG. 9. Experimental angular distributions for $l = 2$ transitions in ^{91}Zr(d, p) (points) in comparison with distorted-wave calculations.

It is interesting that the proposed $(\frac{11}{2})^-$ assignment for the state near 2.16 MeV from inelastic scattering is consistent with the stripping results.

B. Residual Nucleus ^{92}Zr

The spectroscopic-factor sums agree well with the theoretically expected values for the $d_{5/2}$, $s_{1/2}$, $d_{3/2}$, and $g_{7/2}$ levels. The sum for $h_{11/2}$ levels is 50% of the total theoretically expected strength, in good agreement with the observed $h_{11/2}$ strength in ^{91}Zr. The other strengths are also in fair to good agreement with the ^{91}Zr results. This suggests that essentially the same single-particle states are observed in the two final nuclei. The separation of the centers of gravity for different subshells agrees with the separations in ^{91}Zr as shown in the last column of Table IV. The values of $\bar{\sigma}$ are smaller than for ^{91}Zr, perhaps contrasting with what one intuitively expects. This may reflect experimental difficulties, since weak transitions in the tail of a distribution of levels dramatically affect the second moment.

The coupling of the stripped neutron to the $\frac{5}{2}^+$ ground state of ^{91}Zr leads to multiplets in ^{92}Zr corresponding to each single-particle level in ^{91}Zr.

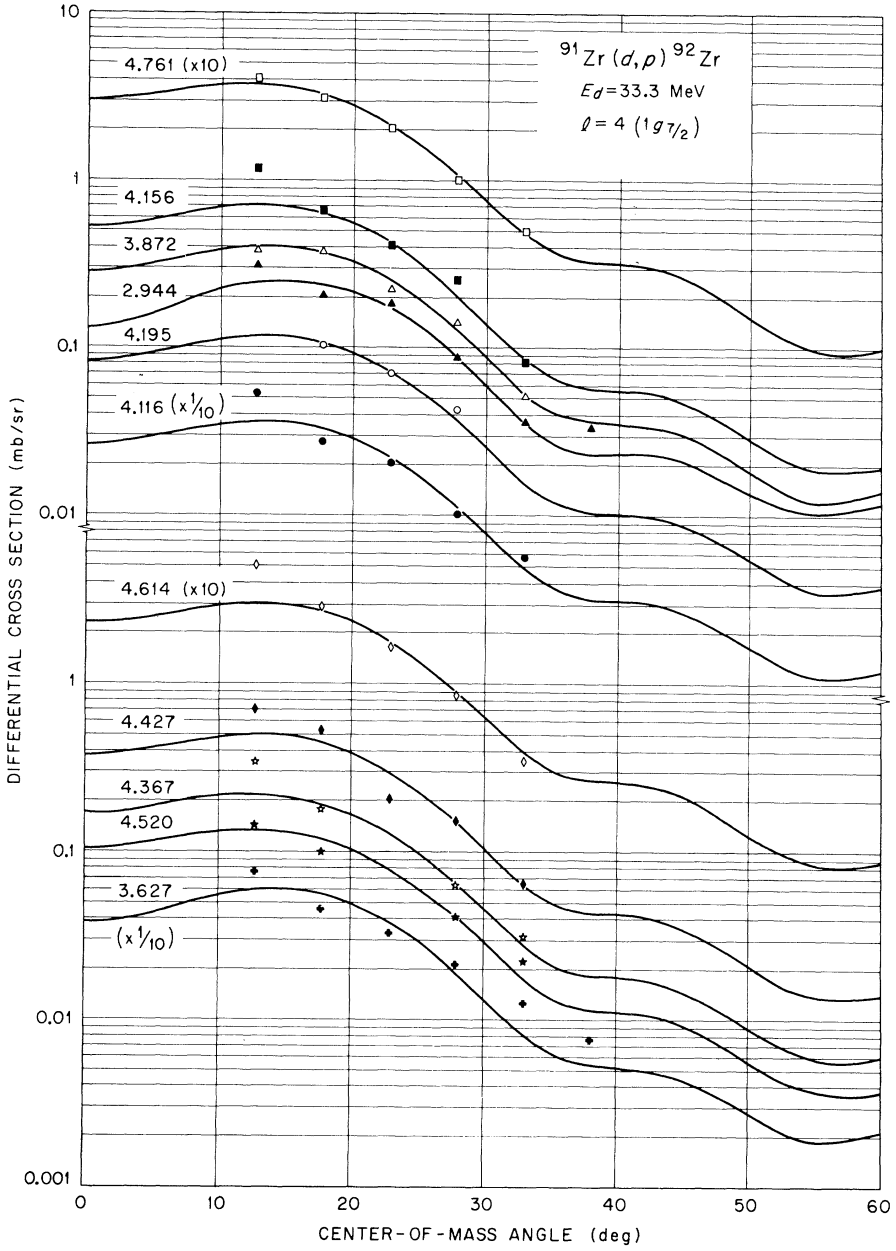

FIG. 10. Experimental angular distributions for $l=4$ transitions in ^{91}Zr(d,p) (points) in comparison with distorted-wave calculations.

TABLE III. Excitation energies, spin assignments, and spectroscopic factors for ^{91}Zr(d,p) and ^{91}Zr$(\alpha, ^3\mathrm{He})$.

^{91}Zr(d,p)					^{91}Zr$(\alpha, ^3\mathrm{He})$	
E^* (MeV)	nl_j	J^π_f	S'	S	E^* (MeV)	S'
0.0	$2d_{5/2}$	0^+	0.316	1.89	0.0	0.19
0.936	$2d_{5/2}$	2^+	1.453	1.74	0.928	1.16
1.385	$2d_{5/2}$	0^+	0.029	0.18		
1.495	$2d_{5/2}$	4^+	3.13	2.08	1.492	2.78
1.844	$2d_{5/2}$	2^+	0.37	0.44	1.836	0.36
2.060	$(3s_{1/2}, 2d_{5/2})$	2^+	(0.36, 0.09[a])	(0.43, 0.11)	2.031	(0.40[a], 0.09)
2.330	$1h_{11/2}$	3^-	0.36	0.31	2.337	0.43
2.390	$(2d_{5/2})$	(4^+)	0.27	0.18	2.41	0.28
2.851	$(2d_{3/2})$		0.41			
2.898	$3s_{1/2}$	3^+	1.07	0.91		
2.944	$(1g_{7/2})$		0.53		2.944	0.48
3.042	$3s_{1/2}$	2^+	0.60	0.72	3.003[b]	0.60[a]
3.110	$(1g_{7/2})$		0.25			0.27
3.174	$1h_{11/2}$		0.53		3.215[b]	1.03
3.223	$1h_{11/2}$		0.64			
3.247	$(2d_{3/2})$		0.22			
3.271	$(3s_{1/2})$		0.4			
3.300	$(2d_{3/2}$		0.4		3.327[b]	0.4[a]
3.357	$(1h_{11/2})$		0.20			0.39
3.453	$2d_{3/2}$		0.67		3.479[b]	0.67[a]
3.490	$(1g_{7/2})$		0.30[c]			0.32[c]
3.581	$1h_{11/2}$		0.93[c]		3.597[b]	1.03[c]
3.627	$(1g_{7/2})$		0.83[c]			0.83[c]
3.685	$(2d_{3/2})$		0.36		3.683[b]	0.62
3.758	$(2d_{3/2})$		0.27			
3.790[b]	$(1h_{11/2}, 2d_{3/2})$		(0.4[a], 0.3)		3.802[b]	(0.37, 0.3[a])
3.872	$1g_{7/2}$		0.78			0.78[a]
3.91	$(1h_{11/2})$		0.20		3.909	0.19
3.989	$2d_{3/2}$		0.87		3.998[b]	0.87[a]
4.022	$(1g_{7/2})$		0.33			0.30
4.065	$2d_{3/2}$		0.90			
4.116	$1g_{7/2}$		0.60			
4.156	$1g_{7/2}$		1.33		4.159[b]	1.63
4.195	$1g_{7/2}$		0.21			
4.367	$(1g_{7/2})$		0.33			
4.427	$(1g_{7/2})$		0.80		4.429	0.79
4.467	$(2d_{3/2})$		0.20			
4.520	$(1g_{7/2})$		0.24			
4.614	$(1g_{7/2})$		0.50		4.600[b]	0.93
4.692	$(2d_{3/2})$		0.25			
4.761	$(1g_{7/2})$		0.60		4.788[b]	0.60[a]
4.799	$(1h_{11/2})$		1.67			1.40
5.265	$(1h_{11/2})$		1.03		5.269	1.03

[a] Arbitrarily fixed to agree with other reaction.
[b] Denotes known doublet.
[c] Corrections were made for contributions from ^{90}Zr impurity.

For a given subshell the number of levels should be $2j+1$ or 6, whichever is smaller, except for $j=\frac{5}{2}$, for which there are only 3 levels because of the Pauli exclusion principle. The relative strengths (S') of the states of a multiplet should vary as $2J_f+1$. By comparison of strengths one may thus be able to deduce the final spin of the ^{92}Zr residual nucleus. However, these single-particle states mix with other configurations, and only a partial success in assignment of spins was realized as indicated below.

The spins of states populated by $d_{5/2}$ are known, and hence one can calculate the spectroscopic factors. The sums of spectroscopic factors for 0^+, 2^+, and 4^+ states below 2.5 MeV are 2.07, 2.39, and 2.26, respectively. These are very close to the expected values of 2.0.

For the states populated by $l=0$ transitions, one

at 2.060 MeV is known to be 2^+ and has a spectroscopic factor of 0.43. Since the theoretically expected sum for 2^+ states is 1.00, it is highly probable that the strongly excited level at 2.898 MeV is a 3^+ state with a spectroscopic factor of 0.91. The state at 3.042 MeV must then be a 2^+ level with a spectroscopic factor of 0.72 and the state at 3.27 3^+ with a spectroscopic factor of 0.34. With this interpretation the spectroscopic factor sums for 2^+ and 3^+ states are 1.15 and 1.25, respectively.

The abundance of levels populated by $d_{3/2}$ and $g_{7/2}$ transitions makes spin assignments impossible. To a large degree this is also true of the $h_{11/2}$ transitions. However, here the model is somewhat simpler because only one large $h_{11/2}$ transition to ^{91}Zr was observed, and the negative parity states produced by $(d_{5/2}\, h_{11/2})$ couplings do not have an abundance of states to mix with. This coupling scheme produces states with spins ranging from 3^- to 8^-. The state at 2.33 is known to be a 3^- state. Its spectroscopic factor is 0.31. The assumption of (4^-) and (5^-) assignments for the levels at 3.174 and 3.223 MeV, respectively, yields a spectroscopic factor of 0.35 for each state. These agree well with the spectroscopic factor of 0.37 for the 2.157-MeV level in ^{91}Zr. None of the other levels fit well into this simple interpretation, so perhaps configuration mixing is important even for the negative-parity states at energies in excess of 3.25 MeV.

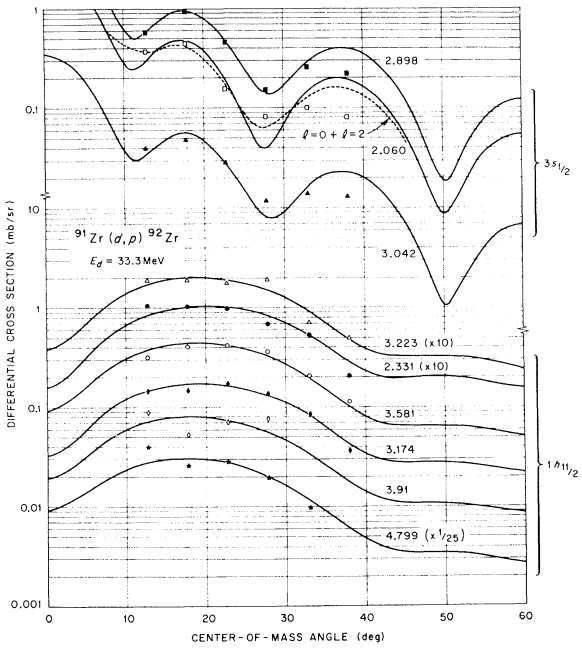

FIG. 11. Experimental angular distributions for $l=0$ and $l=5$ transitions in ^{91}Zr(d,p) (points) in comparison with distorted-wave calculations (smooth curves).

TABLE IV. Summary of results for single-particle levels in ^{91}Zr and ^{92}Zr.
The expected spectroscopic-factor sums are based on the assumption that the $N=50$ shell is closed.

		^{90}Zr$(d,p)^{91}$Zr				^{91}Zr$(d,p)^{92}$Zr				
		$\sum S_j(i)$				$\sum S'_j(i)$				
nl_j	Number of transitions	Expected	Measured	ϵ_j (MeV)	$\bar{\sigma}_j$ (MeV)	Number of transitions	Expected	Measured	ϵ_j (MeV)	$\bar{\sigma}_j$ (MeV)	$\epsilon_j(91)-\epsilon_j(90)$ (MeV)
$2d_{5/2}$	2	1.00	1.07	0.04	0.24	7	5.00	5.66	1.41	0.52	1.37
$3s_{1/2}$	3	1.00	1.37	1.66	0.67	4	2.00	2.43	2.87	0.36	1.21
$2d_{3/2}$	8	1.00	1.51	2.76	0.71	11	4.00	4.85	3.75	0.45	0.99
$1g_{7/2}$	4	1.00	1.07	2.77	0.66	14	8.00	7.63	4.04	0.49	1.27
$1h_{11/2}$	5	1.00	0.58	2.68	0.82	9	12.00	5.96	4.08	0.89	1.40

ACKNOWLEDGMENTS

We are indebted to J. B. Ball for many valuable discussions and for instructions on the proper use of the spectrograph, and to Darla Patterson, Mia Armitage, and William Prater for scanning the plates.

*Research supported by The Army Research Office-Durham under a grant to the University of Tennessee and by the U. S. Atomic Energy Commission under contract with Union Carbide Corporation.

[1]B. L. Cohen and O. V. Chubinsky, Phys. Rev. 131, 2184 (1963).

[2]C. E. Brient, E. L. Hudspeth, E. M. Bernstein, and W. R. Smith, Phys. Rev. 148, 122 (1966).

[3]J. K. Dickens, F. G. Perey, and R. J. Silva, in *International Conference on Nuclear Physics, Gatlinburg, 1966,* edited by R. L. Becker, C. Goodman, P. H. Stelson, and A. Zucker (Academic Press, Inc., New York, 1967).

[4]J. K. Dickens and E. Eichler, Nucl. Phys. A101, 408 (1967).

[5]G. Simmestad, M. Iverson, and J. J. Kraushaar, Technical Progress Report, University of Colorado Nuclear Physics Laboratory, Report No. COO-535-603, 1969 (unpublished).

[6]C. R. Bingham, M. L. Halbert, and R. H. Bassel, Phys. Rev. 148, 1174 (1966).

[7]C. R. Bingham and M. L. Halbert, Phys. Rev. C 1, 244 (1970).

[8]E. Newman, L. C. Becker, B. M. Preedom, and J. C. Hiebert, Nucl. Phys. A100, 225 (1967).

[9]M. P. Fricke, E. E. Gross, B. J. Morton, and A. Zucker, Phys. Rev. 156, 1207 (1967).

[10]J. B. Ball, IEEE Trans. Nucl. Sci. 13, 340 (1966).

[11]W. Whaling, in *Handbuch der Physik,* edited by S. Flügge (Springer-Verlag, Berlin, Germany, 1958), Vol. 34, pp. 193–217.

[12]Program developed by R. M. Drisko, R. H. Bassel, and G. R. Satchler.

[13]R. H. Bassel, R. M. Drisko, and G. R. Satchler, Oak Ridge National Laboratory Report No. ORNL-3240, 1962 (unpublished).

[14]C. R. Bingham and M. L. Halbert, Phys. Rev. 158, 1085 (1967).

[15]R. H. Bassel, private communication.

[16]T. K. Lim, Bull. Am. Phys. Soc. 14, 1222 (1969).

[17]F. G. Perey and A. M. Saruis, Nucl. Phys. 70, 225 (1965).

[18]J. K. Dickens, R. M. Drisko, F. G. Perey, and G. R. Satchler, Phys. Letters 15, 337 (1965).

[19]J. B. Ball and C. B. Fulmer, Phys. Rev. 172, 1199 (1968).

[20]G. R. Satchler, private communication.

[21]J. L. DuBard and R. K. Sheline, Phys. Rev. 182, 1320 (1969).

PHYSICAL REVIEW C VOLUME 2, NUMBER 6 DECEMBER 1970

Alpha-Decay Studies of the $N = 127$ Isotones ^{214}Fr, ^{215}Ra, and ^{216}Ac†

David F. Torgerson and Ronald D. Macfarlane*

Department of Chemistry and Cyclotron Institute, Texas A & M University, College Station, Texas 77843

(Received 11 August 1970)

The study of nuclei which are one neutron removed from the $N = 126$ closed shell has shown that the odd-proton $N = 127$ isotones α decay from both the ground state and a metastable state whose excitation energy decreases between ^{210}Bi and ^{216}Ac. The α-decay daughters of these nuclei show some correspondence in their energy-level spacings which is due to the coupling of specific single-particle configurations near the $N = 126$ closed shell. New information has been obtained for the α decay of the 1− isomer of ^{214}Fr to levels in ^{210}At, and for the α decay of ^{216}Ac to levels in ^{212}Fr. The decay scheme of ^{216}Ac is markedly different from that reported by others. An experimental and theoretical study of the α decay of ^{215}Ra has also been made.

I. INTRODUCTION

Experimental investigations of the $N = 125$ and $N = 127$ isotones near the ^{208}Pb core are particularly interesting because of the relative simplicity of the states at low excitation energy. Theoretical[1-4] and experimental[5-8] studies of the energy levels of ^{208}Bi and ^{210}Bi have shown the importance of a residual neutron-proton tensor component in the shell-model force. It has also been demonstrated experimentally that the qualitative features of this interaction are retained at low excitation energies when proton pairs are added to these nuclei.[8-12]

The odd-proton $N = 127$ isotones ^{210}Bi, ^{212}At, and